

General Disclaimer

One or more of the Following Statements may affect this Document

- This document has been reproduced from the best copy furnished by the organizational source. It is being released in the interest of making available as much information as possible.
- This document may contain data, which exceeds the sheet parameters. It was furnished in this condition by the organizational source and is the best copy available.
- This document may contain tone-on-tone or color graphs, charts and/or pictures, which have been reproduced in black and white.
- This document is paginated as submitted by the original source.
- Portions of this document are not fully legible due to the historical nature of some of the material. However, it is the best reproduction available from the original submission.

DRA/MARSHALL

(NASA-CR-174332) COMPUTATIONAL FLUID
MECHANICS UTILIZING THE VARIATIONAL
PRINCIPLE OF MODELING DAMPING SEALS Interim
Report (Continuum, Inc.) 26 p HC A03/MF A01

N85-17325

Unclas

CSCI 20D G3/J4 17112

COMPUTATIONAL FLUID MECHANICS UTILIZING
THE VARIATIONAL PRINCIPLE OF MODELING DAMPING SEALS

Interim Report, Contract No. NAS8-35508

CI-IR-0080

Prepared for:

National Aeronautics and Space Administration
George C. Marshall Space Flight Center
Marshall Space Flight Center, AL 35812

By:

J. Michael Abernathy
Richard Farmer

CONTINUUM, Inc.
4715 University Drive, Suite 118
Huntsville, AL 35805

February 7, 1985

SUMMARY

An analysis for modeling damping seals for use in Space Shuttle main engine turbomachinery is being produced. Development of a computational fluid mechanics code for turbulent, incompressible flow is required. This document is an interim report on the first year of work. It was prepared at Continuum, Inc. for NASA-MSFC under Contract NAS8-35508.

ORIGINAL CONTAINS
COLOR ILLUSTRATIONS

TABLE OF CONTENTS

SUMMARY	1
INTRODUCTION	1
THEORY	2
MODEL EVALUATION	11
CLOSURE	19
REFERENCE	19

TABLE OF FIGURES

Fig. 1	Turbulent Boundary Layer Calculation	9
Fig. 2a	Pipe Flow Calculated Using Artificial Compressibility	13
Fig. 2b	Pipe Flow Calculated Using Artificial Compressibility	13
Fig. 3a	Cylinder In Crossflow, Inviscid	14
Fig. 3b	Cylinder In Crossflow, Inviscid	14
Fig. 4a	Cylinder In Crossflow, Viscous	15
Fig. 4b	Cylinder In Crossflow, Viscous	15
Fig. 5	Axisymmetric Pipe Flow With Air	16
Fig. 6	Axisymmetric Pipe Flow With Water	18

INTRODUCTION

One of the limiting factors in the operation of the Space Shuttle main engine (SSME) is the speed of the turbopumps. The turbopumps currently operate near the whirl instability speed. Further increases in SSME thrust will require an increase in this speed. It has recently been suggested that the creation of turbulence in the leakage flow of the current seals would provide additional damping for the rotor. This idea was investigated analytically in Ref. 1. The current work is to use numerical methods to model these damping seals and thus provide a tool to further analyze this concept.

In order to describe the flow in a damping seal, a variational method (known as the VAST code, **V**ariational **S**olution of **T**ransport equations) will be used to solve the governing equations. The VAST code was developed at Continuum, Inc. based on the work of Prozan (Refs. 2,3). For this work Prozan solved the compressible form of the equations, and used the ideal gas equation of state. The investigation of the damping seals requires an incompressible flow solver with liquid as the working fluid.

Incompressible flow solution codes are almost universally implicit in nature. In most codes pressure is generally obtained by solving one of the momentum equations, or by a Poisson equation. Attempts to develop explicit pressure solutions are primarily characterized by the artificial compressibility of Chorin (Ref. 4). Recent applications of this method to the SSME have been demonstrated (Refs. 5,6).

In developing an incompressible version of the VAST code, a pressure solution which falls within the framework of the variational statement is required. A first attempt to include an explicit pressure solution in VAST was made by Farmer (Ref. 7). This procedure utilized one of the momentum equations to basically treat gravity flows, but this causes the code to be directionally biased. This method generally gives different answers if different paths of integration are used (Ref. 8).

In describing the damping seal, the pressure is one of the most critical variables, whereas many of the aforementioned codes use pressure simply as a means of arriving at velocities. Indeed, some researchers have eliminated pressure entirely in their incompressible solutions, as in Ref. 9 or as with the stream function - vorticity formulation.

In the following work, efforts at obtaining a pressure solution that fits the requirements of the damping seal model, and the subsequent development and evaluation of the VAST code for incompressible flows is described. Since the flow in the seals is turbulent, turbulence models must also be included in the code. Thus, work supporting turbulent boundary layer modeling is also discussed. Some results are presented and remaining work is outlined.

THEORY

In the current approach to obtain a solution to the incompressible problem, the general form of the compressible Navier-Stokes equations are initially considered. Thus, the continuity and momentum equations are, respectively:

$$\iiint \frac{\partial \bar{\rho}}{\partial t} dV + \iint \bar{\rho} \bar{V} \cdot d\bar{s} = 0 \quad (1)$$

$$\iiint \frac{\partial (\bar{\rho} \bar{V})}{\partial t} dV + \iint (\bar{\rho} \bar{V}) \bar{V} \cdot d\bar{s} + \iint (\bar{I} \bar{P} - \bar{\tau}) \cdot d\bar{s} = 0 \quad (2)$$

for a single species and neglecting body forces. The energy equation can be used if temperature changes are desired. However, since an incompressible code is sought, the energy equation decouples from Eqs. (1) and (2) so that this extension is straightforward. For simplicity, only the isothermal case is considered here.

In the usual form for incompressible flow, Eq. (1) is written as

$$\iint \bar{V} \cdot d\bar{s} = 0 \quad (3)$$

This equation implies an infinite wave propagation speed. Consequently, any type of truly unsteady, explicit solution to the governing system of equations is precluded. Because of the nature of the damping seals problem, it is desirable to obtain a set of equations that will allow unsteady analyses.

Pressure Equations

Several methods for obtaining accurate pressure for incompressible problems have been studied. One of the most widely used methods is the Poisson equation (Ref. 8). The differential form of this equation is

$$\nabla^2 P = S_P \quad (4)$$

where S_P is a function of the velocities as well as the first three derivatives of the velocities. Reference 8 provides a detailed presentation of Eq. (4), along with stability considerations and boundary conditions. Eq. (4) can only be solved implicitly, although it may be combined with explicit solutions of Eq. (2) and used iteratively to obtain some time varying solutions.

Another solution procedure which has been examined is the penalty function method. An excellent review of this method is given in Ref. 10; however, this procedure is also implicit, and in its usual form is a true finite element formulation. The variational procedure, on the other hand, consists of both finite element and finite difference characteristics, with the actual time integration being carried out with differencing schemes.

A new approach which was considered for this problem was the use of mechanical energy. Since minimum kinetic energy is a known variational principle for some special cases of incompressible flow (Refs. 9,11), it was hoped that this approach could be utilized. The mechanical energy is:

$$\iint \bar{P} \bar{V} \cdot d\bar{s} = - \iiint \frac{\partial (.5\rho V^2)}{\partial t} dV - \iint [(.5\rho V^2) \bar{V} - \bar{\tau} \cdot \bar{V}] \cdot d\bar{s} \quad (5)$$

As with the previously discussed methods, it is seen that there is no time-dependent pressure term once again dictating an implicit solution. Furthermore, Eq. (5) does not actually provide new information beyond Eq. (2), and there is no a priori satisfaction of continuity, while Eq. (4) does satisfy continuity in the form of Eq. (3).

One of the earliest attempts to develop explicit pressure equations for incompressible codes was the artificial compressibility of Chorin (Ref. 4). This work was restricted to steady problems, and had the drawback that the assumed compressibility had no basis in physical reasoning, but rather played the role of a relaxation parameter. Recent work by Chang and Kwak (Ref. 5) and Kwak, et al (Ref. 6) have furthered the applicability of this procedure. The continuity equation can be obtained in the form

$$\iint \frac{\partial P}{\partial t} dv + \beta \iint \bar{V} \cdot d\bar{s} = 0 \quad (6)$$

The explicit nature of the equation is readily apparent, and β is the artificial compressibility coefficient. Again, β is a term introduced for convenience, although in Ref. 5 some theoretical bounds are developed by using an artificial speed of sound and by introducing artificial waves. These bounds are also dependent upon the type of numerical differencing scheme used (Ref. 5). Nonetheless, the procedure was applied successfully to some significant flow problems, including some SSME applications. An attempt to develop a time-accurate solution was also made in Ref. 6 by replacing zero on the right hand side of Eq. (6) with another pressure term and iterating. This procedure, however, is still in the developmental stage.

Although the form and ease of application of Eq. (6) is very appealing, the lack of physical reasoning to obtain the equation, as well as the trial and error procedure often necessary to determine an acceptable value of β , detracts from its usefulness. This deficiency has been overcome by the work of Kawahara and Hirano (Ref. 12). This analysis will not be presented here, but rather a very similar approach which parallels their work is presented. Differences in the resulting pressure equation will then be pointed out.

The initial step in the derivation is to obtain an equation of state. The idea of a limited compressibility is used and the assumed functional form of the equation of state is

$$P = P(\rho) \quad (7)$$

For a liquid (or gas, also), the bulk modulus of elasticity expresses the compressibility of the fluid,

$$E = \frac{dP}{\frac{d\rho}{\rho}} \quad (8)$$

The finite acoustic speed in a liquid is given by

$$c^2 = \frac{E}{\rho} \quad (9)$$

Hence, for all fluids with a finite acoustic speed (which in actuality encompasses all fluids), Eqs. (7), (8), and (9) may be used to write the equation of state as

$$dP = c^2 d\rho \quad (10)$$

For most of the following work, Eq. (10) is used in the differential form wherever possible. However, in some instances it is necessary to integrate this equation with respect to some reference state. This reference state, P_r and ρ_r , must be taken to be the usual theoretical incompressible values of P and ρ for the fluid being considered.

If the integrated form of Eq. (10) is substituted into the continuity equation, Eq. (1), the result, after some manipulation, is

$$\iiint \frac{\partial P}{\partial t} dV + \iint P \bar{V} \cdot d\bar{s} + (\rho_r c^2 - P_r) \iint \bar{V} \cdot d\bar{s} = 0 \quad (11)$$

Note that in this equation, the only appearance of density is the reference density ρ_r . Eq. (11) is a physically meaningful explicit pressure equation. If the quantity

$$(P - P_r) \iint \bar{V} \cdot d\bar{s} \quad (12)$$

is subtracted from the left hand side of Eq. (11), the resulting equation will be identical to the method of Ref. 12. Equation (11) is also very similar to the artificial compressibility equation. If β of Eq. (6) is replaced by $\rho_r c^2 - P_r$ and the $P \bar{V} \cdot d\bar{s}$ term is neglected, the equations become the same. As with artificial compressibility, it is also noted that as the acoustic speed, c , approaches infinity, Eq. (11) reduces to the incompressible continuity equation, Eq (3).

In solving for the momentum, Eqs. (2), the incompressible density, ρ_r , is directly substituted for ρ . A first order analysis indicates that this assumption is valid, however, more study is required.

Turbulence Modeling

The primary direction of work for turbulent flow modeling has been the development of shear stress wall functions for use in the VAST code which will permit viscous analyses without requiring an excessive number of computational grid points. It is impractical to resolve the flowfield in the vicinity of the wall with enough grid points to accurately calculate the wall friction. Wall functions are commonly used to provide the required boundary conditions; however, care must be exercised in order not to make the wall functions too empirical. The end result is to predict frictional losses from the detailed flow vectors, not from the mean channel flow. The following procedure was developed and tested with geometrically simple problems to provide the necessary CFD tools for SSME analysis.

For turbulent wall flows for a smooth wall, including fully developed pipe flows, the following empirical velocity profiles are valid:

$$u^+ = 5.5 + 2.5 \ln(y^+) \quad \text{for } y^+ > 30 \quad (13)$$

$$u^+ = -3.05 + 5.0 \ln(y^+) \quad \text{for } 5 < y^+ < 30 \quad (14)$$

$$u^+ = y^+ \quad \text{for } y^+ < 5 \quad (15)$$

where

$$u^+ = u/u^*$$

$$u^* = (\tau_o/\rho)^{0.5}$$

$$y^+ = (\tau_o/\rho)^{0.5} y/\nu$$

Blasius' empirical shear stress relationship is appropriate.

$$\tau_o = 0.0255 \rho u^2 (\nu/u^* \ell)^{0.25} \quad (16)$$

where $\ell = R$ for pipe flow

$\ell = \delta$ for boundary layers

The boundary layer thickness implied by Eq. (16) and a 1/7 power-law profile is

$$\delta = 0.376 X/R_N^{0.2} \quad (17)$$

From Eq. (15)

$$\left(\frac{\partial u}{\partial y_w}\right) = \tau_o/\rho = (u^*)^2/\nu \quad (18)$$

In terms of real distance from the wall, Eq. (13) represents most of the boundary layer, therefore the following computational procedure is suggested. A fictitious wall is assumed to be 0.0005 ft away from the real wall, and no flow is assumed to occur between the two walls. Equation (13) is valid at .0005 ft from the wall; hence, if u is calculated with a slip boundary condition, u^* is determined. Equation (18) is used to calculate the velocity gradient at the wall. Since Eq. (13) is not explicit in u^* , the approximation

$$u^* = 0.1662529 u^{0.867325} / (y/\nu)^{0.132675} \quad (19)$$

is used. These equations determine the velocity gradient and shear stress at the wall. An eddy viscosity is used to determine both the local shear stress and the variation of this stress with distance from the wall, y .

$$\mu_T = 0.07 u^* \rho (FR) + \mu \quad (20)$$

where

$$\begin{aligned} FR &= (y/0.3 \ell) \quad \text{for } 0 < (y/\ell) < 0.3 \\ FR &= 1.0 \quad \text{for } (y/\ell) > 0.3 \end{aligned}$$

Equations (19) and (20) and the momentum equations were used to calculate the turbulent boundary layer over a flat plate between one and two ft running length over the plate. A turbulent boundary layer was assumed at the leading edge of the plate. The flow was air with a free stream velocity of 100 fps (this is an approximate Reynolds Number of 10^6). By adjusting the constants in Eqs. (19) and (20), the profile at the end of the plate was predicted to be that shown in Fig. 1. The fit is very good, especially near the wall; the calculated wall shear stress is within 5% of the correct answer. This procedure is accurate enough to extend its development to more geometrically complex flows. The reasons for the necessity of adjusting the constants in Eqs. (19) and (20) and for the lack of better fit at y 's near the free stream side of the boundary layer are still under investigation.

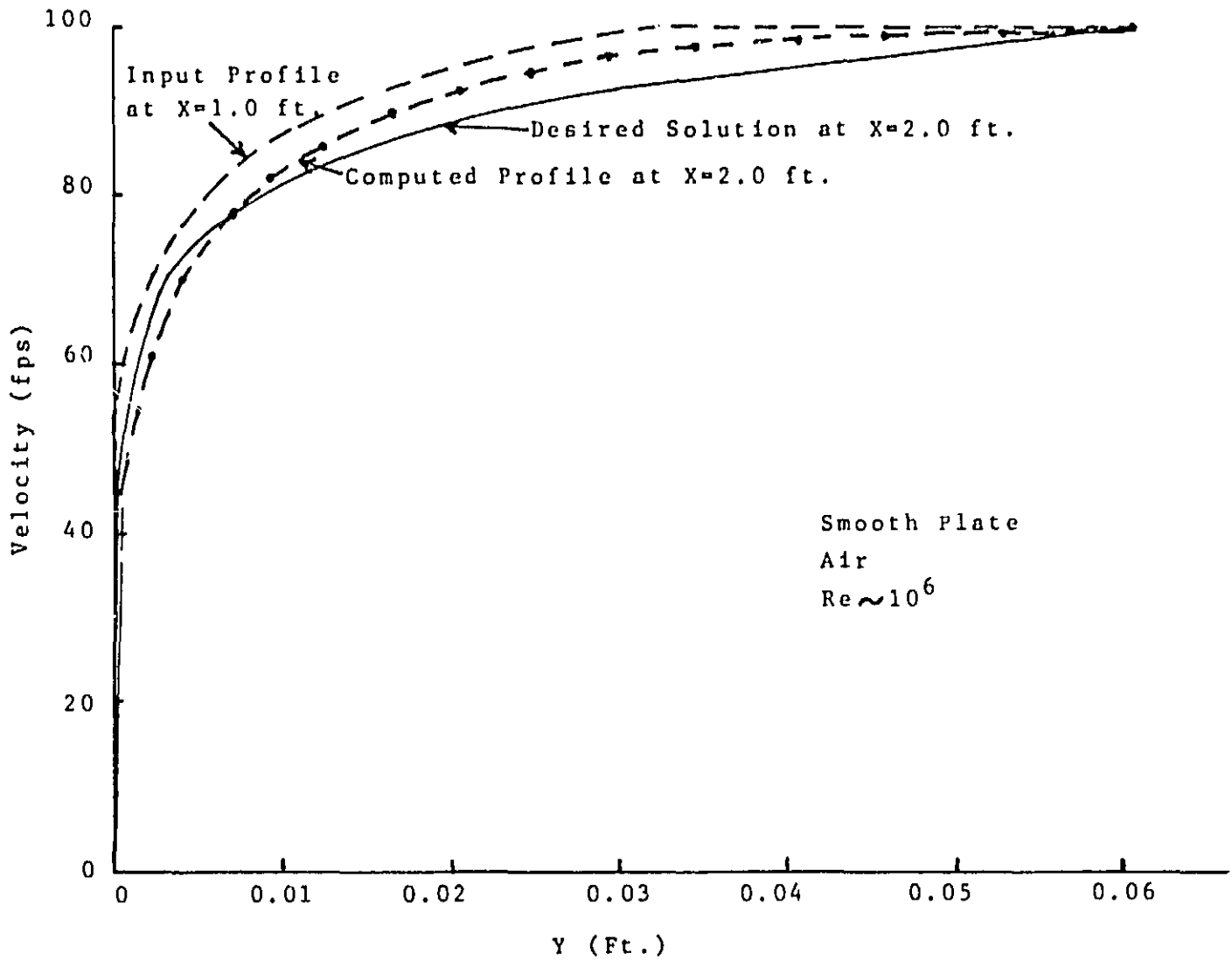


Fig. 1 Turbulent Boundary Layer Calculation

Solution Procedure

In order to use the variational approach developed by Prozan (Refs. 2,3), the governing equations, including the pressure equation must be obtainable from a functional. Functionals are already known for some special cases of incompressible flow (Ref. 11), generally employing the kinetic energy. However, since limited compressibility is used in at least two of the pressure equations previously developed, the entropy functional was used to retain as much commonality as possible with the earlier developments by Prozan.

Beginning with the entropy equation

$$dS = \frac{1}{T} \{dE + PdV\} \quad (21)$$

the differential form of the equation of state, Eq. (10), may be used and, after integration, the entropy functional is obtained as

$$\rho S = c_v \ln T + \frac{1}{T} \left[P + \rho c^2 \ln \left(c^2 - \frac{P}{\rho} \right) \right] + \text{const.} \quad (22)$$

Now, P , u and v are the independent variables, and partial derivatives of Eq. (22) with respect to each of the independent variables are needed. For the velocity derivatives, a velocity-pressure relation is required, and Bernoulli's incompressible relation is assumed.

The derivatives are then derived as

$$\frac{\partial(\rho S)}{\partial P} = \frac{c_v \ln T}{c^2} + \frac{\ln \left(c^2 - \frac{P}{\rho} \right)}{T} \quad (23)$$

$$\frac{\partial(\rho S)}{\partial(\rho u)} = -\frac{u}{T} \left[1 - \frac{c^2}{c^2 + .5 v^2} \right] \quad (23)$$

$$\frac{\partial(\rho S)}{\partial(\rho v)} = -\frac{v}{T} \left[1 - \frac{c^2}{c^2 + .5 v^2} \right]$$

Although Eq. (22) is developed specifically for the pressure equation as given by Eq. (11), the analogous development for the artificial compressibility scheme, Eq. (6), is made by simply using the equation of state developed for this method. (See Refs. 4 and 5 for this equation of state).

The system of equations, Eq. (2), coupled with the preferred pressure equation, can now be solved numerically with the use of proper boundary conditions. Boundary conditions will be discussed in more detail in the next section. Equations (23) are used to prescribe the numerical scheme when Eq. (11) is used for the pressure. Similar procedures are used when alternate pressure equations are employed.

MODEL EVALUATION

The various pressure solutions discussed in the previous section were evaluated for possible use in the damping seals analysis. The mechanical energy equation, Eq. (5) and penalty function methods were eliminated early, primarily due to the implicit nature of the equations. Mechanical energy also suffers from other deficiencies as previously pointed out, particularly with regard to the satisfaction of continuity. The most promising approaches are the Poisson equation and the use of artificial or limited compressibility.

The use of a Poisson equation to obtain pressures is widely known and numerous applications with different numerical codes are thoroughly discussed in Ref. 8. Thus, this solution has not been programmed in the VAST code; however, it will be considered as an alternate procedure to compare various pressure solutions. Its deficiencies for the damping seals analysis are the inefficient iterative procedure for time dependent, three-dimensional solutions and the requirement of Neuman boundary conditions.

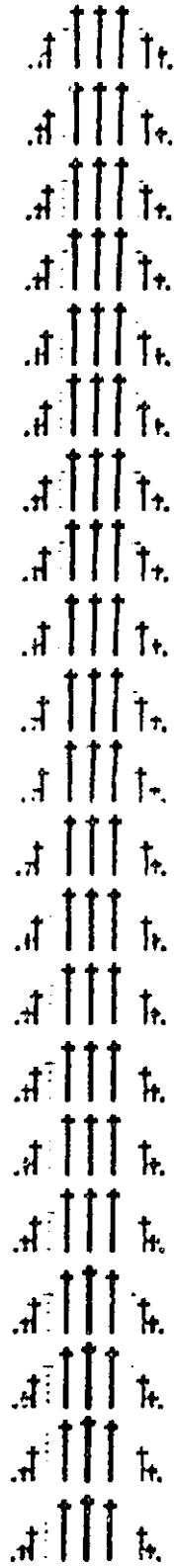
The artificial compressibility method, Eq. (6) was programmed with the VAST code for evaluation. Results for low Reynolds number flows presented in Ref. 6 were good. Since an identical equation was used in the VAST code, only high Reynolds number cases were examined, the majority of time with liquid (water) as the working fluid. For pipe flow, the velocities generally developed well, but not completely. However, pressures were never correct within the pipe and, in fact, showed more of a lateral variation than the

requisite axial dependence. Results for $\beta = 1650$ are shown in Fig. 2. This value showed the best results of six different values between 1.0 and 8100. Because of the dynamic differencing procedure of the VAST code, limits for β , which according to Ref. 5 are dependent on the numerical scheme, could not be accurately developed. Hence a trial and error procedure was necessary. The parameter β also appeared in the variational functional. This led to a low level of confidence in the ability of the functional to accurately dictate the differencing schemes. Due to these problems, it was deemed that the artificial compressibilities pressure solution should not be used if another procedure was found to be adequate.

To attempt to overcome the problems of existing pressure solution methods, the procedure represented by Eq. (11) was developed. Results for both inviscid and viscous flow have been obtained. For a cylinder in a crossflow (half-plane) the inviscid solution is shown in Fig. 3. This figure is for a comparatively fine grid of 1,008 elements; a grid consisting of 224 elements was also run. The results for the fine grid were closer to the analytical solution, although both cases were qualitatively good. The fine grid was run in an effort to produce better results just downstream of the cylinder. Although the streamlines can be shown to be good, the magnitudes of velocities and the pressures are seen to be less than expected. This is believed to be partially due to the initial conditions, which were the assumption of the uniform freestream velocity and pressure everywhere, including the node immediately behind the cylinder.

Several sets of boundary conditions were also investigated for this problem. The conditions used to produce the results of Fig. 3 were: slip walls for the cylinder, centerline, and top of the grid, static pressure on the downstream boundary, and velocities (magnitude and direction) at the upstream boundary. One boundary condition which has not yet been investigated, but which could possibly solve the downstream flow discrepancy, is the use of constant pressure gradient normal to the cylinder surface. This condition, however, would eliminate one advantage of this procedure over a Poisson equation.

Viscous flow over the cylinder was also studied with the course grid. Reynolds numbers of 1.6×10^4 and 1.6×10^5 were run with laminar viscosity values. Results of both cases were good, with those of the higher R_N shown in Fig. 4. The separation and recirculation behind the cylinder are quantitatively very good. Pressure distribution is also correct. Boundary conditions similar to those of the inviscid case were used; however, surface



BETA = 1650

Velocity Scale: 800 - 3900 fps

Fig. 2a Pipe Flow Calculated Using Artificial Compressibility

ORIGINAL PAGE
COLOR PHOTOGRAPH



PRESSURE
AT STEP
6000
ELAPSED TIME
0.1519E-01

5000.

4950.

4900.

4850.

4800.

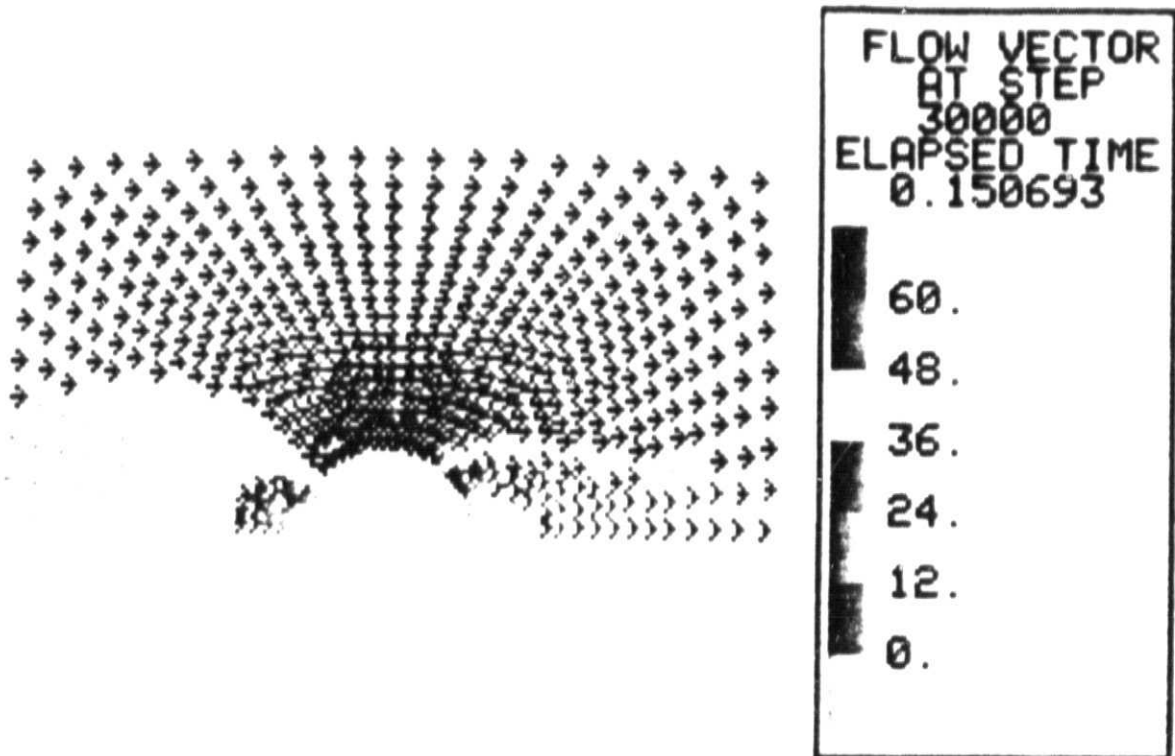
4750.

BETA = 1650

Fig. 2b Pipe Flow Calculated Using Artificial Compressibility, Concluded

ORIGINAL
BLACK AND WHITE PHOTOGRAPH

CYLINDER IN CROSSFLOW, INVISCID



DETAIL NEAR CYLINDER DIRECTIONS ONLY

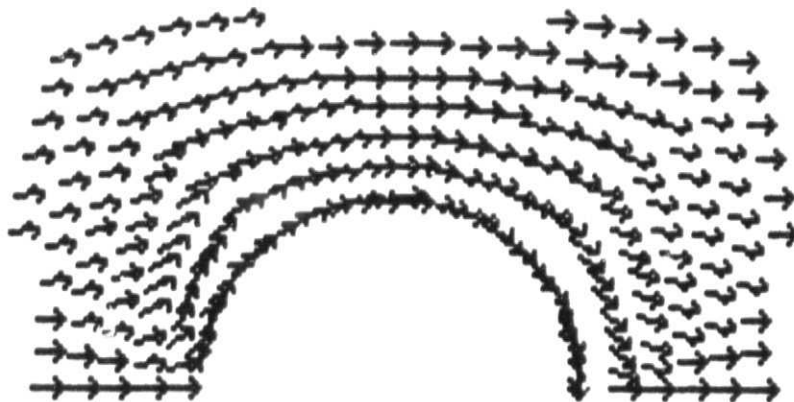
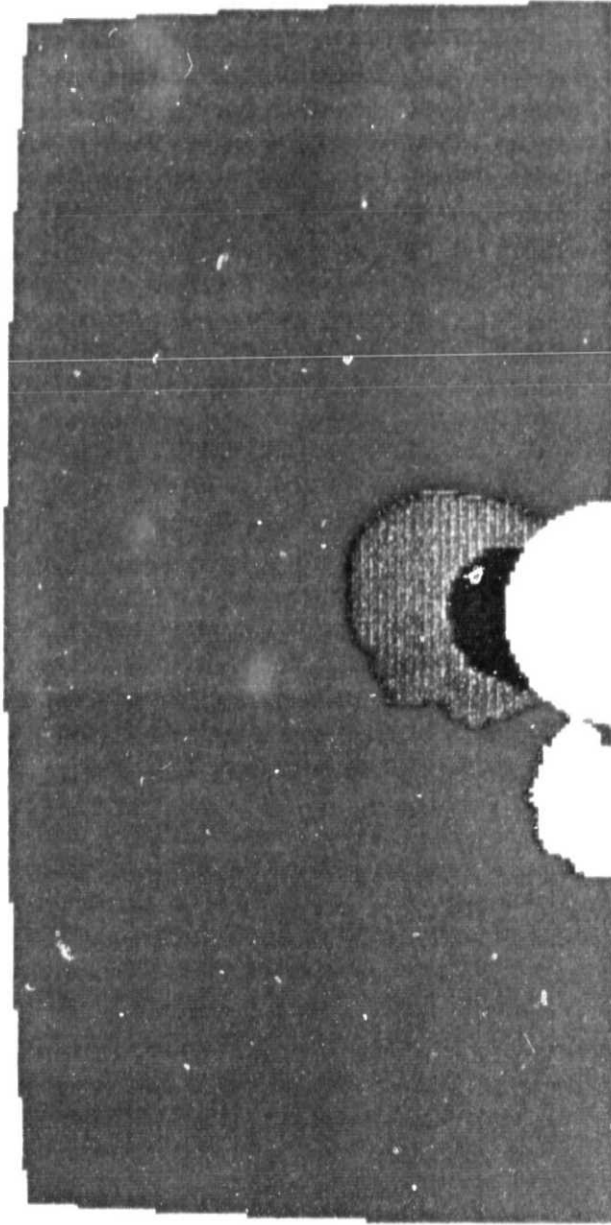


Fig. 3a Cylinder In Crossflow, Inviscid

ORIGINAL PAGE
BLACK AND WHITE PHOTOGRAPH

ORIGINAL PAGE
COLOR PHOTOGRAPH

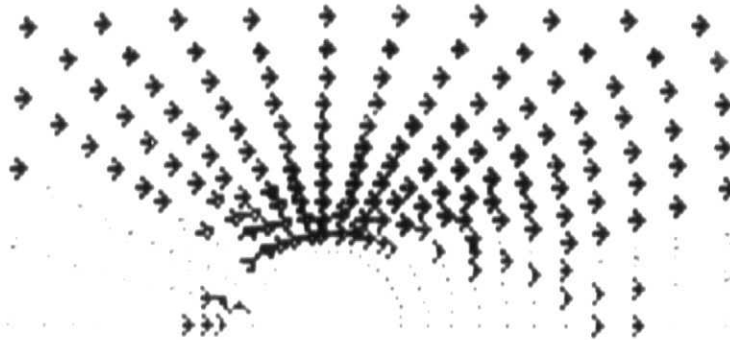
CYLINDER IN CROSSFLOW, INVISCID



PRESSURE AT STEP 30000	ELAPSED TIME
0.150693	2121.
	2119.
	2117.
	2115.
	2113.
	2111.

Fig. 3b Cylinder In Crossflow, Inviscid, Concluded

CYLINDER IN CROSSFLOW, VISCOUS
RN = 1.6E5



FLOW VECTOR
AT STEP
3500
ELAPSED TIME
0.1991E-01

60.
48.
36.
24.
12.
0.

A vertical color scale legend for the flow vector plot. It consists of a vertical bar with a gradient from black at the bottom to white at the top. The scale is labeled with numerical values: 0, 12, 24, 36, 48, and 60. The values increase from bottom to top.

RECIRCULATION DETAIL
FLOW DIRECTIONS ONLY

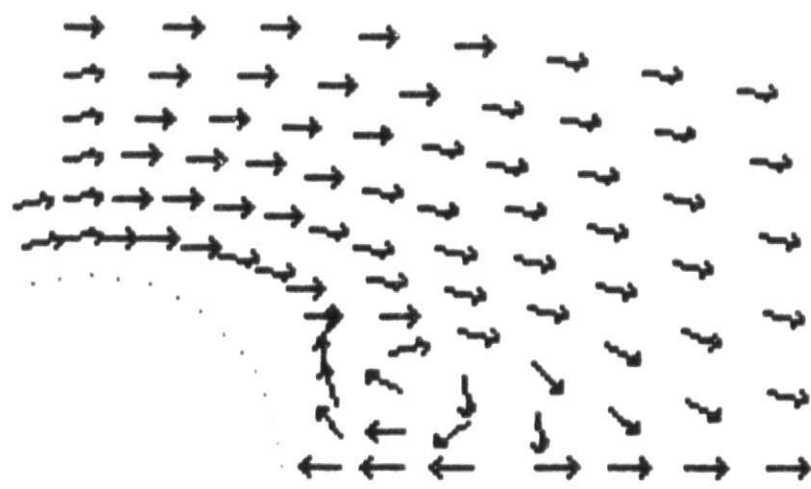
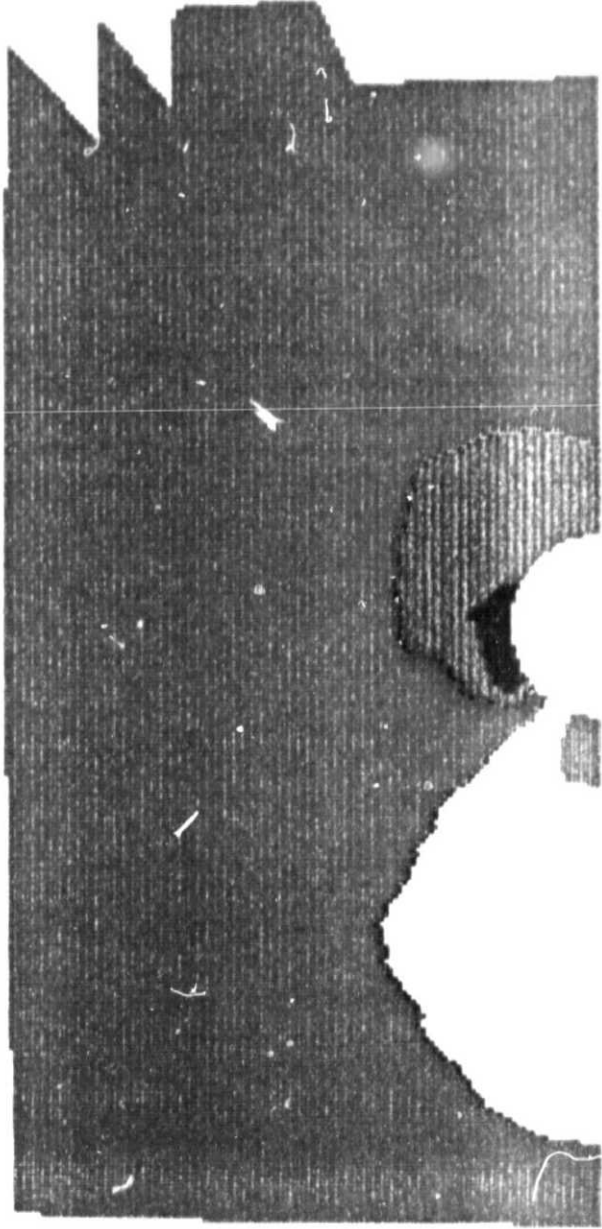


Fig. 4a Cylinder In Crossflow, Viscous

ORIGINAL PAGE
COLOR PHOTOGRAPH

CYLINDER IN CROSSFLOW, VISCOUS

$RN = 1.6E5$



PRESSURE AT STEP	3500
ELAPSED TIME	0.1991E-01
	2121.
	2119.
	2117.
	2115.
	2113.
	2111.

Fig. 4b Cylinder In Crossflow, Viscous, Concluded

ORIGINAL PAGE
BLACK AND WHITE PHOTOGRAPH

AXISYMMETRIC PIPE FLOW , RN = 1000

VELOCITY VECTORS (FRONT HALF OF PIPE)



VELOCITY SCALE: 0 - 240 Ft/sec

VELOCITY VECTORS (REAR HALF OF PIPE)



PRESSURE (ENTIRE PIPE)



PRESSURE AT STEP 16200 ELAPSED TIME 0.1471E-02
2175.
2165.
2155.
2145.
2135.
2125.

Fig. 5 Axisymmetric Pipe Flow With Air

force which was suggested in Ref. 12 was not used. It is expected that this condition would improve the already good solution.

Pipe flow problems, both two-dimensional and axisymmetric, have also been studied. Results for air flow (axisymmetric) at $R_N = 1000$ are shown in Fig. 5. The velocity profile developed well, though not completely, and the pressure is seen to be essentially a function of axial distance alone, as it should be. The predicted pressure drop of approximately 24 psf compares well to the analytical value of 21.4 psf for this problem. This problem has not reached steady state, and further integration should improve the accuracy.

With water as the fluid, pipe flow results were not as encouraging. For a Reynolds number of 2.78×10^5 , the velocities, shown in Fig. 6, are developing well, though slowly. The pressure solution is poor, however. The distribution varies axially, as opposed to the artificial compressibility, but pressure decreases in the upstream direction and even takes on large negative values. Although this problem is not fully understood, the $\rho_r c^2$ term of Eq. (11) completely dominates for this flow (10^4 times as large as the P and P_r terms). The large velocity derivatives produced at the early time steps then effectively swamp the pressure solution. Methods of alleviating this problem other than developing realistic initial profiles with small gradients are under study. Boundary conditions are also being investigated as a potential source of error. The surface force equation (slightly modified) of Ref. (12) was used as the downstream boundary condition. Mass flow and normal pressure gradient boundary conditions could also be required for the pipe problem. However, the slowly developing solution may simply not yet be close enough to steady-state; this possibility is also being investigated further.

In summary, the pressure solution given by Eq. (11) shows promise, but it has not been developed sufficiently. However, it does appear to be the best method if an accurate pressure field is desired. The only alternative is a Poisson equation. Long run times seem to be associated with both methods, as the small CFL produced by the high acoustic speeds of liquids requires many integration steps for the explicit pressure solution. One important result of the success achieved with Eq. (11) for the pressure was the performance of the entropy functional as a variational principle. Although the principle was hypothesized and used for compressible, ideal gases, no stability problems were

ORIGINAL PAGE
COLOR PHOTOGRAPH

AXISYMMETRIC PIPE FLOW, WATER, RN = 2.78E5

VELOCITY, FRONT HALF



VELOCITY SCALE : 0 - 240 FPS

VELOCITY, REAR HALF



PRESSURE, FRONT HALF



PRESSURE, REAR HALF

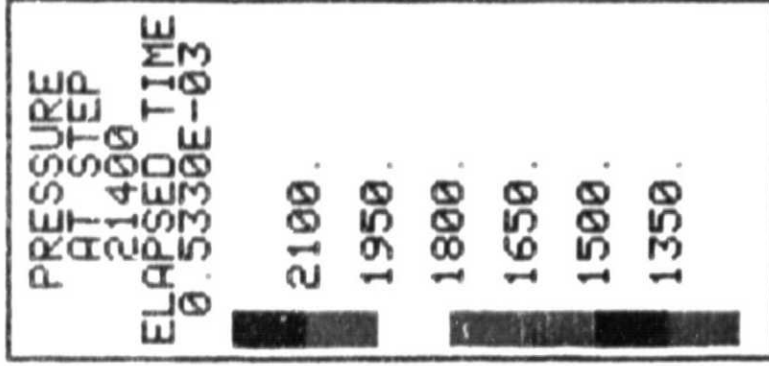


Fig. 6 Axisymmetric Pipe Flow With Water

encountered for the incompressible cases run. This is certainly a factor in pursuing Eq. (11) as the best pressure solution.

CLOSURE

Once the pressure equation has been sufficiently developed, the main obstacle to the damping seals analysis will have been cleared. Eccentric operation and three-dimensional solutions are straightforward extensions of the VAST code. Roughness effects can be handled empirically by the turbulence model developed as Eqs. (19) and (20). Transport equation models are also under evaluation. Damping seals parametric cases can then be studied.

REFERENCES

1. von Pragenau, G.L., "Damping Seals for Turbomachinery", NASA TP 1987, 1982.
2. Prozan, R.J., "A Variational Principle for Compressible Fluid Mechanics, Discussion of the One-Dimensional Theory," NASA CR-3526, April 1982.
3. Prozan, R.J., "A Variational Principle for Compressible Fluid Mechanics, Discussion of the Multi-Dimensional Theory", NASA CR-3614, October 1982.
4. Chorin, A.J., "A Numerical Method for Solving Incompressible Viscous Flow Problems", J. of Computational Physics, vol. 2, 1967, pp. 12-26.
5. Chang, J.L.C. and Kwak, D., "On the Artificial Compressibility for Numerically Solving the Pressure Field of Incompressible Flows", AIAA Paper No. 84-252, 22nd Aerospace Sciences Meeting, Reno, Nevada, January 1984.
6. Kwak, D., Chang, J.L.C., Shanks, S.P. and Chakravarthy, S., "An Incompressible Navier-Stokes Flow Solver in Three-Dimensional Curvilinear Coordinate Systems Using Primitive Variables", AIAA Paper No. 84-253, 22nd Aerospace Sciences Meeting, Reno, Nevada, January 1984.
7. Farmer, R.C., "Mercury-Cadmium-Telluride Crystal Growth Investigation: Solidification Simulation", Final Report on NASA Contract NAS8-35049, June 1983.
8. Roache, P.J., Computational Fluid Mechanics, Hermosa Publishers, Albuquerque, N.M., 1982.

9. Ecer, A., "Variational Formulation of Viscous Flows", Int. J. for Numerical Methods In Engineering, vol. 15, 1980, pp. 1355-1361.
10. Hughes, T.J.R., Liu, W.K. and Brooks, A., "Finite Element Analysis of Incompressible Viscous Flows by the Penalty Function Formulation", J. of Computational Physics, vol. 30, 1979, pp. 1-60.
11. Finlayson, B.A., The Method of Weighted Residuals and Variational Principles, Academic Press, New York, 1972.
12. Kawahara, M. and Hirano, H., "A Finite Element Method for High Reynolds Number Viscous Fluid Flow Using Two Step Explicit Scheme", Int. J. for Numerical Methods In Fluids, vol. 3 1983, pp. 137-163.